DOI: 10.3969/j. issn. 1673-5188. 2016. S1. 001
http://www.cnki.net/kcms/detail/34.1294.TN.20161208.1003.002.html, published online December 8, 2016

Substrate Integrated Waveguide Based Monopulse Slot Antenna Arrays for 60 GHz Applications

ZHU Jianfeng[1, 2], XUE Quan[1, 2], and LIAO Shaowei[1, 2]
(1. State Key Laboratory of Millimeter Waves, City University of Hong Kong, Kowloon, Hong Kong SAR, China;
2. CityU Shenzhen Research Institute, Shenzhen 518057, China)

Abstract

Monopulse slot antenna arrays based on substrate integrated waveguide (SIW) are proposed for the application of 60 GHz monopulse tracking systems in this paper. The sum-difference monopulse comparator can provide a high amplitude and phase balance over wide frequency band and no phase delay technique is required for the difference channel. Resonant slot antennas are adopted as the radiating elements since they can be integrated with the sum-difference monopulse comparator in a single layer with a compact size. Two monopulse arrays with 2 × 4 and 4 × 4 slot elements are designed, fabricated, and measured. Measured results show that the proposed antenna arrays have wide bandwidth covering the unlicensed 60-GHz band. The peak sum beam gain is 13.85 dBi for the 2 × 4 element array and 16.24 dBi for the 4 × 4 element array. The peak difference beam gain is 11.20 dBi for the 2 × 4 element array and 12.11 dBi for the 4 × 4 element array and the maximum null depth can reach -40 dB.

Keywords

resonant slot antenna array; monopulse; substrate integrated waveguide (SIW); millimeter-wave (mmWave)

1 Introduction

The monopulse technique, which compares a signal received simultaneously from the sum (Σ) and difference (Δ) channels, is widely used in millimeter wave radar and satellite systems for target tracking [1]. Monopulse antennas can be simply realized by changing the phases of different radiating elements. The sum beam is achieved when radiating elements are all excited in phases, while two difference beams are obtained by employing an 180-degree phase-shifting to excite several elements. The former can generate one main lobe along the target direction, and the latter exhibits a null in the same direction.

Basically, the monopulse antenna consists of two parts: the monopulse comparator and the radiating elements. The comparator is utilized to generate the sum and difference patterns and the radiating antenna can be planar or three-dimensional (3-D). The 3-D monopulse antennas are usually in a form of reflector antennas, such as Cassegrain parabolic antennas and horn antennas with waveguide monopulse comparators [2], [3]. Though these antennas can obtain good characteristics, the antennas and corresponding monopulse comparator are usually complicated and bulky in structure. Microstrip-based antennas are attractive for monopulse applications due to their low cost and compact size. Various microstrip monopulse antennas have been proposed with good performance [4]–[7]. However, the microstrip technique is inappropriate for V-band applications as the loss of the microstrip structure cannot be neglected at high frequencies. Substrate integrated waveguide (SIW) technology has been demonstrated as a low-loss and high-integration technique for passive components. Till now, several SIW monopulse antenna arrays have been presented [8]–[11]. A substrate integrated monopulse antenna array for W-band was proposed in [8] with good performance, low cost and easy fabrication, but the design complexity is relatively high. LIU et al. [9] proposed a two dimensional SIW monopulse slot antenna array without any microstrip structures. However, the bandwidth of the array is narrow and it suffers from phase imbalance, which results in the deterioration of antenna performance. A SIW monopulse antenna array with filtering respond was proposed in [10], where the comparator was achieved by a square dual-mode SIW cavity resonating at its TE_{201} and TE_{102} modes. A low-profile antenna array combines the scanning capabilities of pillbox configurations and enhanced resolution of two-quadrant monopulse technique was realized in [11].

To overcome these challenges, a SIW-based monopulse slot

This project is supported by the National Basic Research Program of China ("973" Program) under Grant No. 2014CB339900 and the National Natural Science Foundation of China under Grant No. 61372056.

antenna array is proposed, which has good characteristics including wide bandwidth, deep null-depth, high radiation efficiency and high port isolation. Besides, there are two additional advantages of the novel design: 1) The phase delays of the feeding network are frequency independent as the SIW magic T of the comparator, which combines the E-plane and H-plane junctions, can be regarded as a 180-degree hybrid. This provides a constant phase difference between the output ports for the difference channel as well as high degree decoupling between the input ports with a wide frequency range. In addition, as the feeding network is entirely implemented with SIW technology, there is no radiation from feeding network. 2) As for fabrication, the radiating elements and the monopulse comparator are implemented in a single layer and can be realized with standard printed circuit board (PCB) technology.

2 Antenna Design

2.1 Design and Evaluation of Monopulse Comparator

In literature, most of the SIW-based sum and difference feeding networks for mmWave frequencies are implemented by 3 dB directional couplers and 90-degree phase shifters. Although these structures can be well-integrated in a single layer, they can only operate in a rather narrow bandwidth. However, the T-junction shows broad impedance bandwidth, and the outputs of the H-plane junction exhibits high amplitude and phase balance while the E-plane junction can exhibit the same amplitude and reverse phase in a rather broad bandwidth. Inspired by this, a single layered sum-difference feeding network is proposed as shown in **Fig. 1**. In this design, Rogers 5880 PCB laminates with a thickness of 0.787 mm and a relative permittivity of 2.2 is used. Both the sum and difference channels are directly fed by the WR-15 waveguide so that additional radiation from the feed discontinuity can be avoided.

As can be seen in Fig. 1, the sum channel (when port 1 is excited) is based on H-plane Tee where the energy flows into the two arms of the SIW with the same amplitude and phase [12]. In order to obtain good impedance matching between the WR-15 waveguide and the SIW, the widths of the short end sections of SIWs are enlarged from 2.7 mm (a_3) to 4.44 mm (a). The width of the SIW is chosen as 2.7 mm (a_3) so that only the dominant mode exists in the SIW over the whole operating frequency band. For the difference channel (when port 2 is excited), the WR-15 waveguide fed is located in the center of the two arms of the SIW and the axis of the WR-15 is parallel to the plane of the E-field vector of the SIW. The energy is coupled from the WR-15 waveguide by means of E-field and then divided into two arms with the same amplitude but 180-degree phase difference naturally [13]. Due to the field symmetry, the isolation between the sum and difference ports is inherently high. It is worth noting that the presence of the cutting slot for the difference port will have little influence on the response of the previous sum channel because of the high isolation. **Fig. 2** shows the E-field current distributions of the comparator when port 1 and port 2 are excited. In order to obtain a good match of the waveguide-SIW transition of both the sum and difference ports, the posts adjacent to the ports need to be carefully optimized. Detailed configuration of the waveguide-SIW transition is shown in Fig. 1b and corresponding dimensions are shown in **Table 1**.

The sum-difference feed network is arranged back-to-back to evaluate its loss, as shown in **Fig. 3**. The simulated and measured S-parameters are shown in **Fig. 4**. As can been seen, both the simulated and measured reflection coefficients (S_{11}) are lower than −10 dB and the insertion loss is around 1 dB for the simulation and 3.6 dB for the measurement. The simulated and measured S_{22} are lower than −15 dB at most of the band. The simulated insert loss is around 0.6 dB and measured loss is about 1.3 dB. Therefore, the measured insert loss of the monopulse feed network is about 2.5 dB for port 1 and 0.65 dB for port 2.

2.2 Design and Measurement of 2 × 4 Slot Antenna Array

Based on the sum and difference feeding network presented in the previous section, one-dimensional monopulse antenna

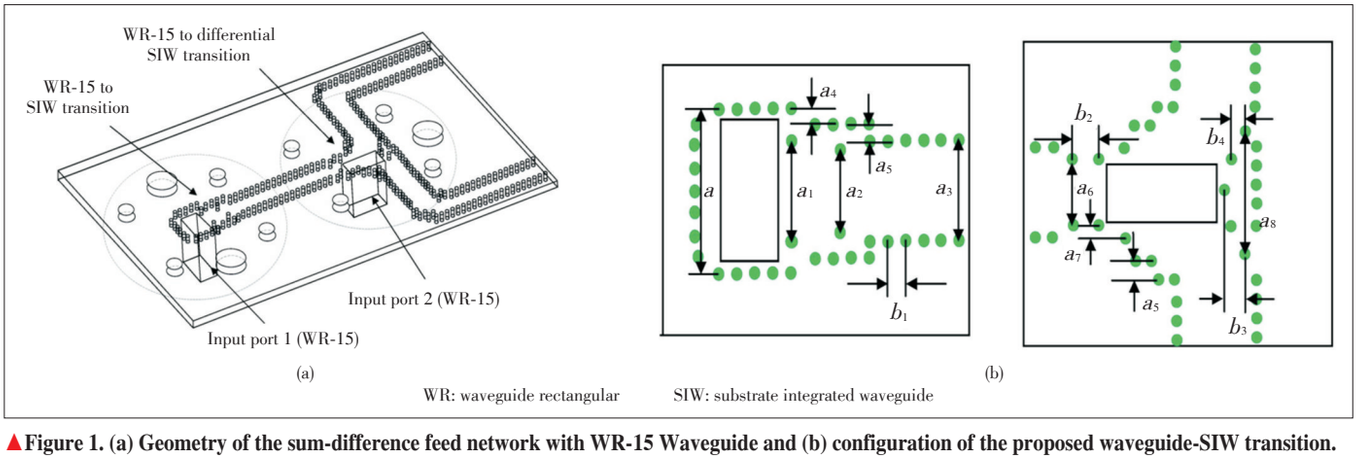

▲**Figure 1. (a) Geometry of the sum-difference feed network with WR-15 Waveguide and (b) configuration of the proposed waveguide-SIW transition.**

arrays with both wide impedance bandwidth and good radiation patterns are presented and discussed. The slot resonant antenna arrays are chosen as the radiating elements because the slot antennas can be well integrated with the feed network. The antennas are simulated by ANSYS High Frequency Structure Simulator (HFSS) [14]. After fabrication, an Agilent network analyzer (E8361A) measures its reflection coefficient. The broadside gain and radiation patterns are measured by an in-house far-field millimeter wave antenna measurement system. Due to the system limitation, only the radiation pattern in the upper half space is measured [15]. The geometry of the 2×4 slot antenna array is shown in **Fig. 5a**. The photograph of the fabricated prototype is shown in **Fig. 5b**.

The simulated and measured reflection coefficients of the 2×4-element slot antenna arrays are given in **Fig. 6**. The measured results show that the reflection coefficients of the arrays are lower than −15 dB at most of the unlicensed 60-GHz band. Moreover, the isolation is better than 20 dB.

The array generates the difference beam in E-plane (*yoz* plane) and the sum beam in both E-plane and H-plane (*xoz* plane) when ports 1 and 2 are excited, respectively. The simulated and measured normalized radiation patterns at 60 GHz are shown in **Fig. 7a** and the results agree well with each other. The null-depth is below −35 dB for the difference beam. The measured sum and difference radiation patterns at 58 GHz and 64 GHz are shown in **Fig. 7b**. The measured maximum gain is 13.85 dBi for the sum beam and 11.2 dBi for the difference beam while the minimum one is 12.1 dBi and 8.8 dBi for the sum beam and difference beam, respectively.

2.3 Design and Measurement of 4×4 Slot Antenna Array

In order to further increase the gain, a 4×4 element array is designed with two two-way equal power dividers, as shown in **Fig. 8**. The two-way power dividers are crucial to the 4×4 antenna array as the

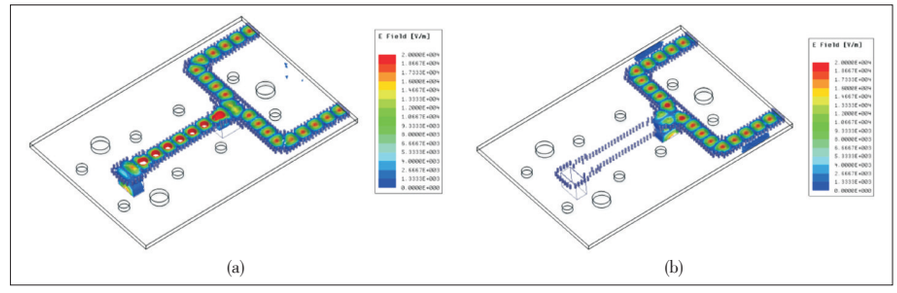

▲**Figure 2. E-field distributions of the comparator when (a) port 1 and (b) port 2 are excited.**

▼**Table 1. Dimensions of the waveguide: SIW transition**

Parameter	a	a_1	a_2	a_3	a_4	a_5	a_6	a_7
Value (mm)	4.44	2.55	2.32	2.70	0.81	0.45	2.10	0.34
Parameter	a_8	b_1	b_2	b_3	b_4			
Value(mm)	3.6	0.6	0.88	0.72	0.42			

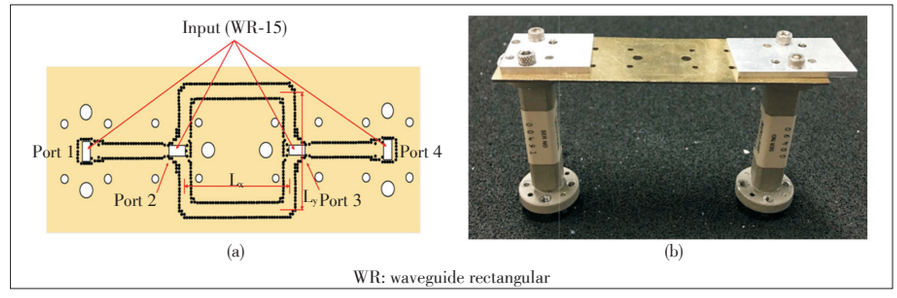

▲**Figure 3. (a) Geometry of the back-to-back test of the simplified differential feeding network (L_x = 24.24 mm and L_y = 19.01 mm) and (b) fabricated prototype.**

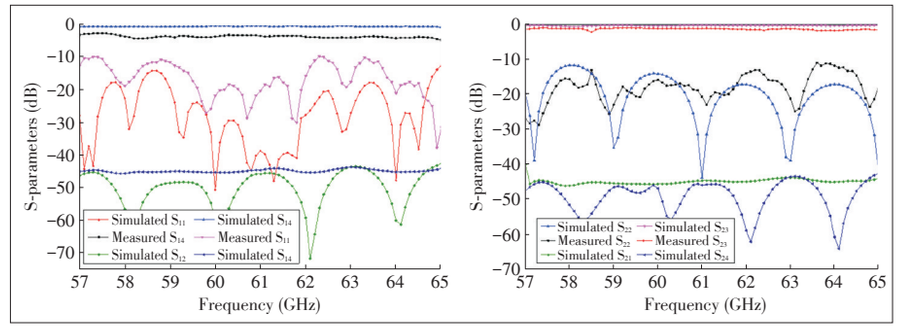

▲**Figure 4. Simulated and measured S-parameters of the back-to-back test of the monopulse feeding network.**

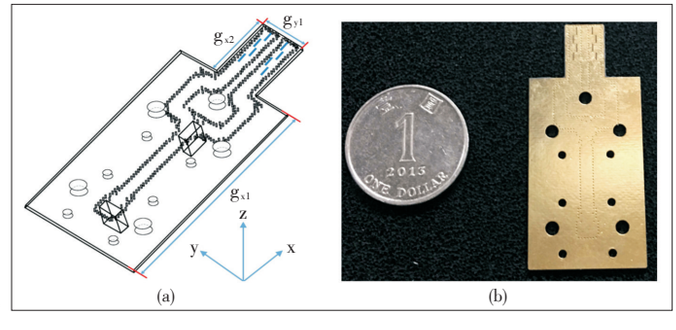

Figure 5. ▶ (a) Geometry of the 2×4 slot antenna array (g_{x1}=39.5 mm, g_{x2}=14.3 mm, g_{y1}=8.7 mm) and (b) the fabricated prototype.

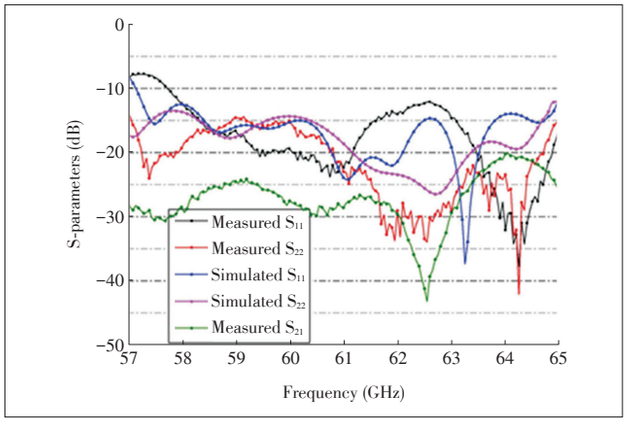

◀**Figure 6. Simulated and measured S-parameters of the 2×4 slot antenna array.**

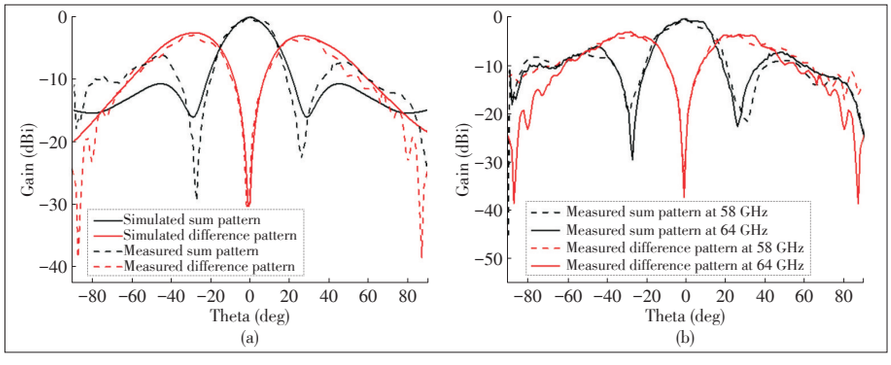

▲**Figure 7. (a) Simulated and measured normalized radiation patterns at 60 GHz and (b) measured sum and difference radiation patterns at 58 GHz and 64 GHz.**

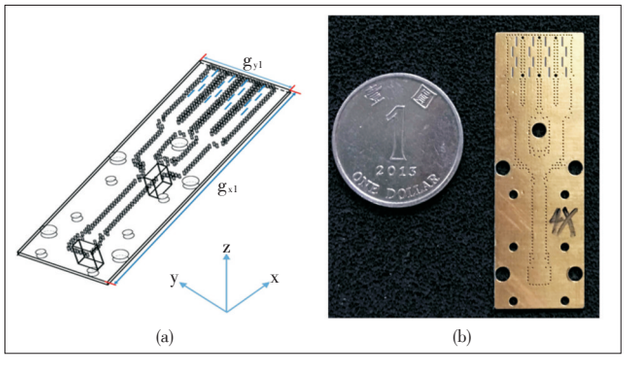

◀**Figure 8. (a) Geometry of the 4×4 slot antenna array (g_{x1}=52.4 mm, g_{y1}=17.7 mm) and (b) the fabricated prototype.**

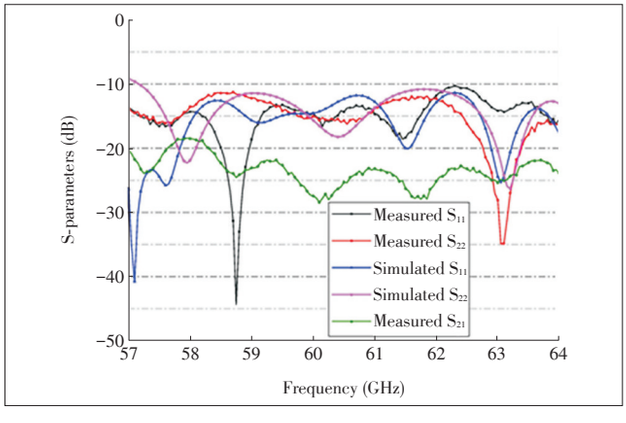

◀**Figure 9. Simulated and measured S-parameters of the 4×4 slot antenna array.**

phase and amplitude imbalance may affect the radiation pattern and antenna gain. Therefore, the power dividers are designed with good impedance matching, high amplitude and phase balance as well as compact size. Simulated results show that from 57 GHz to 65 GHz the input reflection coefficient of the power divider is lower than −18 dB and the phase and amplitude imbalance of the output ports are less than 0.2 dB and 0.6°, respectively.

The simulated and measured reflection coefficients of the 4×4-element arrays are given in **Fig. 9**. The measured results show that the reflection coefficients of the arrays are lower than −10 dB in the entire unlicensed 60-GHz band and the isolation is better than 20 dB.

The 4×4 slot antenna array generates the difference beam in E-plane (*yoz* plane) and the sum beam in both E-plane and H-plane (*xoz* plane) when port 1 and port 2 are excited, respectively. The simulated and measured normalized radiation patterns at 60 GHz are shown in **Fig. 10a** and the measured sum and difference radiation patterns at 58 GHz and 64 GHz are shown in **Fig. 10b**. The null-depths are both below −28 dB for the difference beam. The measured maximum gain is 16.24 dBi for the sum beam and 12.11 dBi for the difference beam while the measured minimum gain is 13.4 dBi and 9.89 dBi for the sum beam and difference beam, respectively.

3 Conclusions

In this paper, SIW-based monopulse slot antenna arrays are proposed for the 60 GHz applications. The monopulse comparator is realized by the combination of the H-plane and E-plane junctions in a single layer. This provides high amplitude and phase balance over a wide frequency band. Based on the monopulse comparator, the 2×4 and 4×4 element slot antenna arrays with compact size are designed, fabricated and measured. The simulated and measured results of the proposed antennas are in good agreement, indicating the antennas are good candidates for future millimeter-wave monopulse systems.

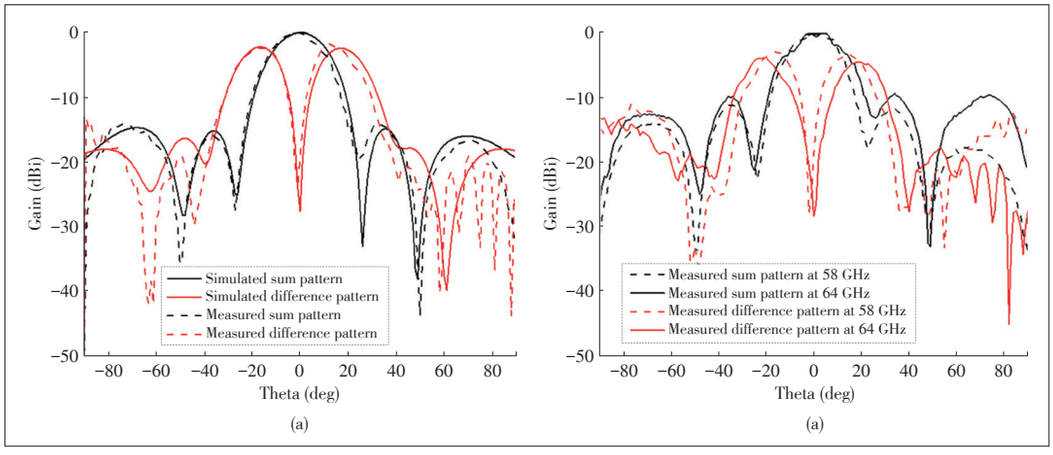

◀Figure 10.
(a) Simulated and measured sum and difference patterns at 60 GHz and (b) measured sum and difference patterns at 58 GHz and 64 GHz.

References

[1] S. M. Sherman and D. K. Barton, *Monopulse Principles and Techniques*. Norwood, USA: Artech House, 2011.

[2] C. E. Profera and L. H. Yorinks, "A high efficiency dual frequency multimode monopulse antenna feed system," *IEEE Transaction on Aerospace and Electronic Systems*, vol. AES - 2, no. 6, pp. 314– 322, Nov. 1966. doi: 10.1109/TAES.1966.4502022.

[3] K. M. Lee and R. S. Chu, "Design and analysis of a multimode feed horn for a monopulse feed," *IEEE Transaction on Antennas and Propagation*, vol. 36, pp. 171–181, Feb. 1988. doi: 10.1109/8.1094.

[4] H. Wang, D.-G. Fang, and X. G. Chen, "A compact single layer monopulse microstrip antenna array," *IEEE Transaction on Antennas and Propagation*, vol. 54, no. 2, pp. 503–509, Feb. 2006. doi:10/1109/TAP.2005.863103.

[5] Y. W. Wang, G. M. Wang, Z. W. Yu, J. G. Liang, and X. J. Gao,"Ultra-wideband e -plane monopulse antenna using vivaldi antenna," *IEEE Transaction on Antennas and Propagation*, vol. 62, no. 10, pp.4961–4969, Oct. 2014. doi:10.1109/TAP.2014.2342767.

[6] S.-G. Kim and K. Chang, "Low-cost monopulse antenna using bidirectionally-fed microstrip patch array," *Electronics Letters*, vol. 39, no. 20, pp. 1428–1429, Oct. 2003. doi: 10.1049/el:20030963.

[7] Z. W. Yu, G. M. Wang, and C. X. Zhang, "A broadband planar monopulse antenna array of c-band," *IEEE Antennas and Wireless Propagation Letters*, vol. 8, pp. 1325–1328, 2009. doi: 10.1109/LAWP.2009.2038077.

[8] Y. J. Cheng, W. Hong, and K. Wu, "94 GHz substrate integrated monopulse antenna array," *IEEE Transaction on Antennas and Propagation*, vol. 60, no. 1, pp. 121–129, Jan. 2012. doi: 10.1109/TAP.2011.2167945.

[9] B. Liu, W. Hong, Z. Kuai, et al., "Substrate integrated waveguide (SIW) monopulse slot antenna array," *IEEE Transaction on Antennas and Propagation*, vol. 57, no. 1, pp. 275–279, Jan. 2009. doi: 10.1109/TAP.2008.2009743.

[10] H. Chu, J. X. Chen, S. Luo, and Y. X. Guo, "A millimeter-wave filtering monopulse antenna array based on substrate integrated waveguide technology," *IEEE Transaction on Antennas and Propagation*, vol. 64, no. 1, pp. 316–321, Jan. 2016. doi: 10.1109/TAP.2015.2497351.

[11] K. Tekkouk, M. Ettorre, L. Le Coq, and R. Sauleau, "SIW pillbox antenna for monopulse radar applications," *IEEE Transaction on Antennas and Propagation*, vol. 63, no. 9, pp. 3918– 3927, Sept. 2015. doi: 10.1109/TAP.2015.2446996.

[12] A. S. Khan, *Microwave Engineering: Concepts and Fundamentals*. Boca Raton, USA: CRC Press, 2014.

[13] S. Liao, P. Wu, K. M. Shum, and Q. Xue, "Differentially fed planar aperture antenna with high gain and wide bandwidth for millimeterwave application," *IEEE Transaction on Antennas and Propagation*, vol. 63, no. 3, pp. 966–977, Mar. 2015. doi: 10.1109/TAP.2015.2389256.

[14] *HFSS Version 15.0.0*, Ansoft Corporation, 2012.

[15] S. Liao, P. Chen, P. Wu, and Q. Xue, "Substrate-integrated waveguide-based 60-GHZ resonant slotted waveguide arrays with wide impedance bandwidth and high gain," *IEEE Transaction on Antennas and Propagation*, vol.63, no. 7, pp.2922–2931, 2015. doi: 10.1109/TAP.2015.2423696.

Manuscript received: 2016-06-15

Biographies

ZHU Jianfeng (zhujianfeng@bupt.edu.cn) received the BS degree in communication engineering from Beijing University of Posts and Telecommunications, China in 2013, where he is currently working toward the PhD degree. Since October 2015, he has been with City University of Hong Kong, China as a research assistant. His research interest is millimeter-wave antennas.

XUE Quan (eeqxue@cityu.edu.hk) received the BS, MS, and PhD degrees in electronic engineering from the University of Electronic Science and Technology of China (UESTC), China, in 1988, 1990, and 1993, respectively. In 1993, he joined the UESTC, as a Lecturer. He became a Professor in 1997. From October 1997 to October 1998, he was a Research Associate and then a Research Fellow with the Chinese University of Hong Kong. In 1999, he joined the City University of Hong Kong where he is currently a Chair Professor of Microwave Engineering. He also serves the University as the Director of Information and Communication Technology Center (ICTC), the Deputy Director of CityU Shenzhen Research Institute, and the Deputy Director of State Key Lab of Millimeter Waves (Hong Kong). He was the Associate Vice President (Innovation Advancement and China Office) from June 2011 to January 2015. He has authored or co-authored over 260 internationally referred journal papers and over 100 international conference papers. His research interests include microwave passive components, active components, antenna, microwave monolithic integrated circuits (MMIC, and radio frequency integrated circuits (RFIC), etc. Professor XUE served the IEEE as an AdCom member of MTT-S from 2011-2013 and the associate editor of *IEEE Transactions on Microwave Theory* and Techniques (2010 - 2013), the associate editor of *IEEE Transactions on Industrial Electronics* (2010-present).

LIAO Shaowei (shaowei.s.liao@ieee.org) received the PhD in electromagnetic fields and microwave technology from UESTC, China in 2010. From October 2007 to September 2009, he was a research assistant in the Department of Electronics, Carleton University, Canada. From January 2011 to August 2011, he was with the School of Electronic Engineering, UESTC, as a lecturer. From September 2011 to July 2012, he served as a senior research associate in the Department of Electronic Engineering, City University of Hong Kong. From July 2012 to September 2013, he joined Bell Labs Research in China, Alcatel-Lucent Shanghai Bell, as a research scientist. Now, he is an engineer at State Key Laboratory of Millimeter Waves, City University of Hong Kong. His research interests include antennas (in particular, millimeter-wave antennas and GNSS antennas), electromagnetic simulation and computational electromagnetics.